

The Orthogonalization of Magnetic Systems

J. M. G. Merayo¹, F. Primdahl^{1,2}, P. Brauer¹, T. Risbo³, N. Olsen² and T. Sabaka⁴

¹Department of Automation, Technical University of Denmark, Building 327, 2800 Lyngby, Denmark

²Danish Space Research Institute, Juliane Maries vej 30, 2100 Copenhagen Oe, Denmark

³Geophysical Department, Copenhagen University, Juliane Maries vej 30, 2100 Copenhagen Ø, Denmark

⁴Geodynamics branch, NASA-GSFC, code 921, Greenbelt, Maryland 20771, USA

Corresponding author's telephone: +45 45 25 34 52, fax: +45 45 88 71 33, email: jmgm@iau.dtu.dk

Abstract

The construction of an orthogonal reference frame based on a set of three skew axes for a magnetic coil system is discussed. For a skew system, it is possible to define the coil axes and the magnetic axes as a dual set of axes that are linked to the system. Therefore, one orthogonal reference frame can be identified from the coil axes and another from the magnetic axes. But there are also other possibilities.

The parametrizations for the magnetic sensors CSC (Ørsted satellite) and CDC (Astrid-2 satellite) are analysed. In principle, only the transformation matrix that orthogonalizes the sensor is needed, but it is customary to express this matrix as function of some non-orthogonal angles. Therefore, most relevant conventions from the literature are presented for comparison. In the case of small angle approximation that is valid for most sensors, they all agree.

Key words: magnetic systems, calibration, instrumentation

1.- INTRODUCTION

The calibration of a magnetometer is a procedure that is usually carried out by instrument builders in order to qualify the magnetometer or by scientists that require the physical information from the instrument. It is important then to understand the operation of the instrument before attempting to describe the relation between its output and the physical quantities.

The NASA satellite MAGSAT (1979-80) was the first dedicated mission to map the Earth's magnetic field vector from space (see Acuña *et al.* 1978). The magnetic instrumentation that was implemented in the satellite was of the Compact Detector Coil (CDC) sensor type. It consisted of three individual fluxgate transducers that provided the vector information of the magnetic field relative to the axes of a star imager (Acuña 1981). A similar sensor geometry has been adapted for the Swedish Auroral microsatellite ASTRID-2 (1998-99), see figure 1a. This magnetometer is described by Brauer *et al.* (1998) and Pedersen *et al.* (1999). This type of sensor (CDC) exhibits a non-linearity due to the large uncompensated transverse fields (Primdahl *et al.* 1992 and Brauer *et al.* 1997).

Twenty years after MAGSAT, the Danish satellite ØRSTED (1999-) is the second dedicated magnetic mapping mission. The magnetic vector measurements are performed by the fluxgate magnetometer that uses the Compact Spherical Coil (CSC) sensor type, see figure 1b, designed by Primdahl and Jensen (1982). The operation principle and employed materials are described by Nielsen *et al.* (1995) and Nielsen *et al.* (1997), respectively. This type of sensor is also used in the German satellite CHAMP (planned for 2000-2005) and the Argentinean satellite SAC-C (planned for 2000-2005) missions.

In the context of this paper, the Compact Spherical Coil (CSC) sensor type will be referred as the CSC-ØRSTED and the Compact Detector Coil (CDC) sensor type as the CDC-ASTRID-2.

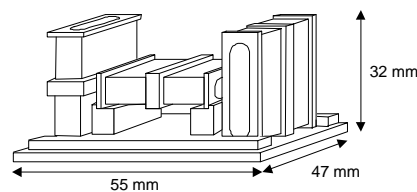


Figure 1a.- The CDC-ASTRID-2 fluxgate sensor for the magnetometer on-board the Astrid-2 satellite. A similar sensor geometry was used in the MAGSAT satellite.

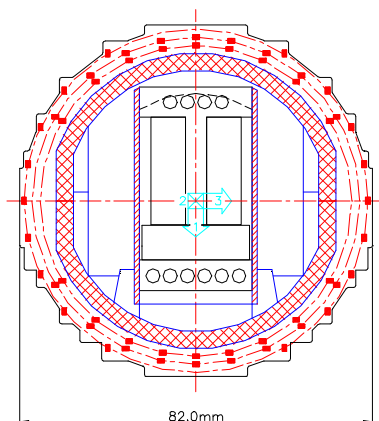


Figure 1b.- The CSC-ØRSTED fluxgate sensor for the magnetometers on-board the Ørsted, SAC-C and CHAMP satellites.

The theory of the scalar calibration method by using the Earth's magnetic field intensity to estimate the calibration parameters of a given vector magnetometer is treated in Merayo (1999B). Because the representation used in describing the CSC-ØRSTED instrument outputs (Merayo *et al.* 2000), differs from that used for that of the CDC-ASTRID-2 (Merayo *et al.* 1999A), based on apparently the same reference sensor system, some concern was raised as to the nature of this discrepancy.

The objective of this paper is to explain in more detail this apparent discrepancy. Hence, by the initiation of a series of definitions the problem is put on a well founded basis. These include the coil axes and the magnetic axes that are used in order to determine an orthogonal reference coordinate system representation.

A second objective, but not less important, is to achieve a common agreement between different groups that are working on similar problems and using different approaches.

2.- The COIL SYSTEM

The magnetic field that is created by a coil of a given geometry depends on the position relative to the coil. If it is assumed that this coil system is large enough, there will be a centre volume in which the field is homogeneous to some level. In general, this volume is small compared to the size of the coil. In theory, a solenoid of infinite length will produce a homogeneous magnetic field inside its boundaries. Also, a spherical coil with constant winding density along the axis would create a homogeneous field inside the sphere (Primdahl and Jensen 1982). This idealized coil will be referred to simply as a *coil* in the rest of this paper.

2.1.-Definition of the coil axes. The *coil axis* is the direction of the magnetic field vector that is produced at the geometrical centre of such a coil when a current is applied to the windings of the coil. If the coil geometry has rotational symmetry, the *coil axis* would be the axis of symmetry. Therefore, when an electric current of intensity I is applied to the coil, the magnetic field produced is proportional to the current and along the *coil axis* \mathbf{c} :

$$\mathbf{B} = s I \mathbf{c} \quad (1)$$

where s in [nT/A] is the proportionality factor and \mathbf{c} is the unit vector that establishes the direction of the coil axis in a specific coordinate system.

In order to allow the possibility of creating magnetic fields in all directions, we must have a set of three coils with a common centre, and whose combination determines the direction and strength of the magnetic field. These coils have their own individual coil axes that are represented by the triad $\{\mathbf{c}_1, \mathbf{c}_2, \mathbf{c}_3\}$. The magnetic field due to the three coils will then be:

$$\mathbf{B} = s_1 I_1 \mathbf{c}_1 + s_2 I_2 \mathbf{c}_2 + s_3 I_3 \mathbf{c}_3 \quad (2)$$

In order to produce a magnetic field along the coil axis \mathbf{c}_1 , a current of magnitude I_1 is applied to the coil with scale factor s_1 . The same occurs for the other two axes \mathbf{c}_2 and \mathbf{c}_3 .

Ideally, the orientation of these coils is arranged in such a way that their coil axes are perpendicular to each other. Nevertheless, in the laboratory this is not possible to achieve, so that in a practical system the axes are slightly skew, deviating from being at right angles to each other.

2.2.- Associating a reference system to the coil axes. An orthogonal reference coordinate system can be associated to the skew coil axes. From these skew coil axes $\{\mathbf{c}_1, \mathbf{c}_2, \mathbf{c}_3\}$, a reference frame based on the orthogonal unit vectors $\{\mathbf{i}^C, \mathbf{j}^C, \mathbf{k}^C\}$ can be constructed. The following equation summarizes this system:

$$\begin{aligned} \mathbf{i}^C &\equiv \mathbf{c}_1 \\ \mathbf{j}^C &\equiv \mathbf{k}^C \times \mathbf{c}_1 = g_1 \mathbf{c}_1 + g_2 \mathbf{c}_2 \\ \mathbf{k}^C &\equiv \frac{\mathbf{c}_1 \times \mathbf{c}_2}{|\mathbf{c}_1 \times \mathbf{c}_2|} = x_1 \mathbf{c}_1 + x_2 \mathbf{c}_2 + x_3 \mathbf{c}_3 \end{aligned} \quad (3)$$

This indicates that the first orthogonal axis \mathbf{i}^C is chosen to be in the direction of the first coil axis, \mathbf{c}_1 . The third orthogonal axis \mathbf{k}^C is perpendicular to the plane defined by the first and second coil axes, \mathbf{c}_1 and \mathbf{c}_2 . In this plane formed by \mathbf{c}_1 and \mathbf{c}_2 , the second orthogonal axis lies, \mathbf{j}^C , and it is perpendicular to \mathbf{c}_1 . This completes the right-handed orthogonal system associated with the triad $\{\mathbf{c}_1, \mathbf{c}_2, \mathbf{c}_3\}$. Therefore in the reference system $\{\mathbf{i}^C, \mathbf{j}^C, \mathbf{k}^C\}$:

$$\begin{aligned}
\mathbf{c}_1 &= \begin{bmatrix} 1 \\ 0 \\ 0 \end{bmatrix} \\
\mathbf{c}_2 &= \begin{bmatrix} -\frac{\mathbf{g}_1}{\mathbf{g}_2} \\ \frac{1}{\mathbf{g}_2} \\ \mathbf{g}_2 \\ 0 \end{bmatrix} = \frac{1}{\sqrt{1-\mathbf{n}_{12}^2}} \begin{bmatrix} -\mathbf{n}_{12} \\ 1 \\ 0 \end{bmatrix} \cong \begin{bmatrix} -\mathbf{n}_{12} \\ 1 \\ 0 \end{bmatrix} \\
\mathbf{c}_3 &= \begin{bmatrix} -\frac{\mathbf{x}_1 + \mathbf{g}_1 \mathbf{x}_2}{\mathbf{x}_3} \\ \frac{\mathbf{g}_2 \mathbf{x}_2}{\mathbf{x}_3} \\ -\frac{1}{\mathbf{g}_2 \mathbf{x}_3} \\ \frac{1}{\mathbf{x}_3} \end{bmatrix} = \frac{\mathbf{x}_3}{1-\mathbf{n}_{12}^2} \begin{bmatrix} \mathbf{n}_{12}\mathbf{n}_{23} & -\mathbf{n}_{13} \\ \mathbf{n}_{12}\mathbf{n}_{13} & -\mathbf{n}_{23} \\ & 1 \end{bmatrix} \cong \begin{bmatrix} -\mathbf{n}_{13} \\ -\mathbf{n}_{23} \\ 1 \end{bmatrix} \\
\mathbf{x}_3 &= \pm \sqrt{\frac{1-\mathbf{n}_{12}^2}{1-\mathbf{n}_{12}^2 - \mathbf{n}_{23}^2 - \mathbf{n}_{13}^2 + 2\mathbf{n}_{12}\mathbf{n}_{23}\mathbf{n}_{13}}} \cong \pm \sqrt{\frac{1-\mathbf{n}_{12}^2}{1-\mathbf{n}_{12}^2 - \mathbf{n}_{23}^2 - \mathbf{n}_{13}^2}} \cong \pm 1
\end{aligned} \tag{4}$$

The construction of the coils is achieved with high precision, although still the axes are slightly skew. In this context the quantities γ_i and ξ_i are used to compute the orthogonal unit vectors from linear combinations of the coils axes unit vectors in equation (3). Therefore, γ_1 , ξ_1 and ξ_2 are very close to zero and γ_2 and ξ_3 are very close to one. The relations between the quantities γ_i and ξ_i to make $\{\mathbf{c}_1, \mathbf{c}_2, \mathbf{c}_3\}$ unit vectors are investigated in Merayo *et al.* (2000) demonstrating that only three quantities v_{ij} , i.e. the cosine function of the angles between the vectors \mathbf{c}_i are sufficient to describe the coil axes with respect the orthogonal system. The quantities v_{ij} equal the angle deviating from the orthogonality in the small-angle approximation.

The magnetic field \mathbf{B} can also be determined in the orthogonal system. In order to find the components of \mathbf{B} in the triad $\{\mathbf{i}^C, \mathbf{j}^C, \mathbf{k}^C\}$, we note that:

$$\mathbf{B} = B_1 \mathbf{i}^C + B_2 \mathbf{j}^C + B_3 \mathbf{k}^C \tag{5}$$

and equation (3) gives the value of the orthogonal basis as function of the coil axes. If equation (5) is then combined with equation (3), the field is expressed as:

$$\begin{aligned}
\mathbf{B} &= B_1 \mathbf{c}_1 + B_2 (\mathbf{g}_1 \mathbf{c}_1 + \mathbf{g}_2 \mathbf{c}_2) + B_3 (\mathbf{x}_1 \mathbf{c}_1 + \mathbf{x}_2 \mathbf{c}_2 + \mathbf{x}_3 \mathbf{c}_3) \\
&= (B_1 + B_2 \mathbf{g}_1 + B_3 \mathbf{x}_1) \mathbf{c}_1 + (B_2 \mathbf{g}_2 + B_3 \mathbf{x}_2) \mathbf{c}_2 + B_3 \mathbf{x}_3 \mathbf{c}_3
\end{aligned} \tag{6}$$

By identifying coefficients from equations (2) and (6), the currents that have to be applied in the coils to produce the given magnetic field components are found. This is written in matrix form where U is an upper triangular matrix. We note that the inversion of an upper triangular matrix is another upper triangular matrix. Thus:

$$\begin{bmatrix} s_1 I_1 \\ s_2 I_2 \\ s_3 I_3 \end{bmatrix} = \begin{bmatrix} 1 & \mathbf{g}_1 & \mathbf{x}_1 \\ 0 & \mathbf{g}_2 & \mathbf{x}_2 \\ 0 & 0 & \mathbf{x}_3 \end{bmatrix} \begin{bmatrix} B_1 \\ B_2 \\ B_3 \end{bmatrix} \equiv U^{-1} \begin{bmatrix} B_1 \\ B_2 \\ B_3 \end{bmatrix} \quad (7)$$

It is also possible to find the relation between the components of the magnetic field and the currents in the coils by inverting (7). This gives the magnetic field components, when a set of currents have been applied to the coils. Hence:

$$\begin{bmatrix} B_1 \\ B_2 \\ B_3 \end{bmatrix} = \begin{bmatrix} 1 & -\mathbf{g}_1 & \mathbf{g}_1 \mathbf{x}_2 - \mathbf{x}_1 \\ 0 & \mathbf{g}_2 & \mathbf{g}_2 \mathbf{x}_3 - \mathbf{x}_2 \\ 0 & 0 & \mathbf{x}_3 \end{bmatrix} \begin{bmatrix} s_1 I_1 \\ s_2 I_2 \\ s_3 I_3 \end{bmatrix} \equiv U \begin{bmatrix} s_1 I_1 \\ s_2 I_2 \\ s_3 I_3 \end{bmatrix} \quad (8)$$

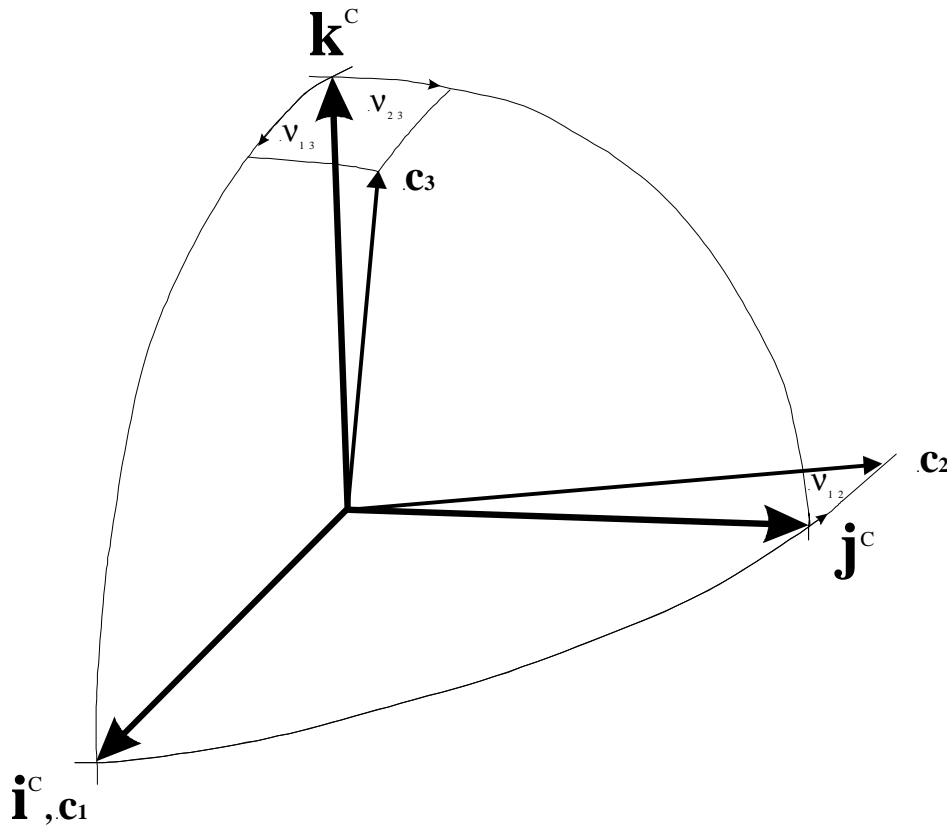


Figure 2.- The coil axes $\{\mathbf{c}_1, \mathbf{c}_2, \mathbf{c}_3\}$ of a skew three dimensional coil system. From these skew axes the orthogonal system $\{\mathbf{i}^c, \mathbf{j}^c, \mathbf{k}^c\}$ can be constructed. The non-orthogonal angles v_{12} , v_{13} and v_{23} are very small.

3.- The FLUXGATE TRANSDUCER

The fluxgate sensor consists of a magnetic core that is driven by an excitation coil and is surrounded by a pickup or detector coil. Several geometries may be devised, but because of its symmetry the ringcore (figure 3) is preferred for space applications. The operation of the fluxgate is based on the changing permeability of a core that lies inside the pickup coil. The core experiences a saturation state twice every cycle of the excitation current. Therefore, the magnetic field inside the core is amplified by the apparent permeability with respect to the value outside the core. Hence, the magnetic field \mathbf{B} inside the detector coil is:

$$\mathbf{B} = (\mu_a - 1)\mathbf{g} \times \mathbf{B}_{\text{ext}} \times \mathbf{g} + \mathbf{B}_{\text{ext}} \quad (9)$$

where μ_a is the time dependent apparent relative permeability of the ringcore, \mathbf{B}_{ext} is the constant ambient magnetic field and \mathbf{g} is a unit vector defining the normal direction of the ringcore plane. The resultant magnetic field is the combination of the amplified field in the plane of the core superposed on the background field \mathbf{B}_{ext} . The demagnetizing factor of the ringcore will be assumed negligible in the plane of the core and very large across this plane, therefore a magnetic field perpendicular to the plane of the ringcore will not cause any effect. Any rotation of the core about the axis \mathbf{g} (yaw angle) would not change the field in the core. However, the output of the magnetic transducer depends on the direction of the magnetic field relative to the sensorial element. The flux seen by the detector coil with a cross-sectional area $\mathbf{A} = A\mathbf{d}$, where \mathbf{d} is the detector axis, would be $\Phi = \mathbf{B} \cdot \mathbf{A}$, thus the voltage induced in the pickup coil is:

$$\begin{aligned} V &= -\frac{d\Phi}{dt} = -A \frac{d}{dt} \{(\mu_a - 1)(\mathbf{g} \times \mathbf{B}_{\text{ext}} \times \mathbf{g}) \cdot \mathbf{d}\} \\ &= -A \frac{d\mu_a}{dt} \{\mathbf{B}_{\text{ext}} \cdot \mathbf{d} - (\mathbf{B}_{\text{ext}} \cdot \mathbf{g})(\mathbf{g} \cdot \mathbf{d})\} \cong -A \frac{d\mu_a}{dt} \mathbf{B}_{\text{ext}} \cdot \mathbf{d} \end{aligned} \quad (10)$$

The angle between the magnetic field \mathbf{B}_{ext} and the detector axis \mathbf{d} is α and the angles defining the normal direction of the ringcore plane \mathbf{g} relative to the detector normal axis (perpendicular to the plane of the detector coil) are θ and ϕ or the roll and pitch angles, respectively. These angles are very small and assumed negligible in the following. Therefore, the sensing component of the core seen by the detector coil is assumed in the plane of the detector coil, i.e. $\mathbf{g} \cdot \mathbf{d} = 0$.

The output of the detector coil can also be the short-circuited current. Moreover, the signal will be proportional to the time varying core permeability as well. This signal contains the magnetic information in the 2nd and higher order even harmonics of the excitation frequency, and these are demodulated in the first stages of the magnetometer electronics. The open loop output of the magnetometer will then be proportional to $\mathbf{B}_{\text{ext}} \cdot \mathbf{d}$. A closed loop feedback system applies a balancing magnetic field to the sensor, so that the electronic demodulator produces zero output. This feedback magnetic field can be produced by an extra coil or by the detector coil itself. But in either way the field set up in the feedback coil projected onto the ringcore plane has to be equal in magnitude (by design it is opposite in direction) to the field

seen by the sensor. For θ and ϕ small, the output of the magnetometer would be proportional to $\mathbf{B}_{\text{ext}} \cdot \mathbf{d}$.

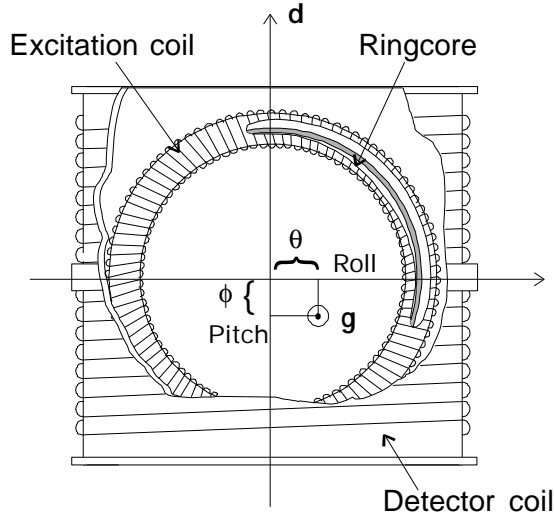


Figure 3.- The ringcore fluxgate transducer. The ring shaped magnetic core is supplied with a toroidal excitation coil. The ring core is surrounded by a flat pick-up or detector coil, and it is placed freely with respect to the detector coil with the pitch, roll and yaw angles θ , ϕ and rotation about \mathbf{g} .

The direction for which the output of the transducer is maximum is defined as the *magnetic axis* of the sensor and it is approximately aligned to the *detector coil axis* \mathbf{d} , as indicated above. In the rest of this paper the unit vectors \mathbf{g} and \mathbf{d} will be considered to be exactly perpendicular to each other. Consequently, the *magnetic axis* of the sensor will be along the *detector coil axis* \mathbf{d} .

4.- The CDC SENSOR for the ASTRID-2 SATELLITE MAGNETOMETER

The Compact Detector Coil (CDC) has been used in the Astrid-2 mission. A sensor of similar geometry was used on the MAGSAT mission. The CDC-ASTRID-2 sensor works in such a manner that each of the individual sensors forming the triaxial system is compensated separately by its own electronics and feedback coil. Under the assumption that the sensors are sufficiently far from each other, so that there is no mutual interaction, each of the detector coils and cores that formed the CDC-ASTRID-2 sensor (see figure 1a) can be assigned a detector axis. Then, we can identify a set of three detector axes $\{\mathbf{d}_1, \mathbf{d}_2, \mathbf{d}_3\}$ that are unit vectors and skew, deviating from being at right angles to each other. When a magnetic field is applied to the sensor, each fluxgate transducer element senses the projection of the magnetic field onto its detector axis, which is determined by the corresponding magnetic core and coil axes. Consequently, each of the electronic channels will create a current that compensates for this projected field and provides zero field condition for each of the individual axes.

Likewise, an orthogonal reference coordinate system may be associated to the skew detector axes $\{\mathbf{d}_1, \mathbf{d}_2, \mathbf{d}_3\}$. Equation (3), (4) and (5) hold if the coils axes \mathbf{c}_i are interchanged with the detector axes \mathbf{d}_i , and the reference system $\{\mathbf{i}^D, \mathbf{j}^D, \mathbf{k}^D\}$ is constructed, i.e. $\mathbf{i}^D = \mathbf{d}_1$, $\mathbf{j}^D = \gamma_1 \mathbf{d}_1 + \gamma_2 \mathbf{d}_2$, $\mathbf{k}^D = \xi_1 \mathbf{d}_1 + \xi_2 \mathbf{d}_2 + \xi_3 \mathbf{d}_3$ and the magnetic field in the

orthogonal system of the sensor is $\mathbf{B}=\mathbf{B}_1\mathbf{i}^D+\mathbf{B}_2\mathbf{j}^D+\mathbf{B}_3\mathbf{k}^D$. The CDC-ASTRID-2 sensor reacts to an external magnetic field \mathbf{B} that is projected onto the individual detector axes \mathbf{d}_i , and eq. (2) is replaced by $s_i I_i=\mathbf{B}\cdot\mathbf{d}_i$ ($i=1,2,3$). Its operation matrix is found by dotting the magnetic field \mathbf{B} into equation (3), so that the relation between the orthogonal components of \mathbf{B} and their projections onto the detector axes is found. If L represents a lower triangular matrix (its inverse is also a lower triangular matrix), the relationship between the components, in matrix notation, can then be written as:

$$\mathbf{B}_{\text{ext}} = \begin{bmatrix} \mathbf{B}_1 \\ \mathbf{B}_2 \\ \mathbf{B}_3 \end{bmatrix} = \begin{bmatrix} 1 & 0 & 0 \\ \mathbf{g}_1 & \mathbf{g}_2 & 0 \\ \mathbf{x}_1 & \mathbf{x}_2 & \mathbf{x}_3 \end{bmatrix} \begin{bmatrix} \mathbf{B}\cdot\mathbf{d}_1 \\ \mathbf{B}\cdot\mathbf{d}_2 \\ \mathbf{B}\cdot\mathbf{d}_3 \end{bmatrix} \equiv L \begin{bmatrix} \mathbf{B}\cdot\mathbf{d}_1 \\ \mathbf{B}\cdot\mathbf{d}_2 \\ \mathbf{B}\cdot\mathbf{d}_3 \end{bmatrix} \quad (11)$$

This means that the relation between the orthogonal components of the external magnetic field \mathbf{B}_{ext} and the outputs from the magnetometer can be expressed by equation (11). In this case, the outputs (in engineering units) of the magnetometer EU_i are proportional to the quantities $\mathbf{B}\cdot\mathbf{d}_i$, as $p_i(EU_i - O_i) = -\mathbf{B}\cdot\mathbf{d}_i$. Thus

$$\mathbf{B}_{\text{ext}} = \begin{bmatrix} 1 & 0 & 0 \\ \mathbf{g}_1 & \mathbf{g}_2 & 0 \\ \mathbf{x}_1 & \mathbf{x}_2 & \mathbf{x}_3 \end{bmatrix} \begin{bmatrix} p_1(EU_1 - O_1) \\ p_2(EU_2 - O_2) \\ p_3(EU_3 - O_3) \end{bmatrix} \equiv A_{CDC} \begin{bmatrix} EU_1 - O_1 \\ EU_2 - O_2 \\ EU_3 - O_3 \end{bmatrix} \quad (12)$$

Inverting equation (11), the *magnetic axes* of the CDC-ASTRID-2 sensor are seen to be the rows of the inverse matrix in equation (11), since the set of three row vectors dotted with the magnetic field, will give the magnetometer outputs. The *magnetic axes* are then the *detector coil axes*.

4.1.- Definition of the orthogonal magnetometer sensor axes for the CDC.

The relation between the orthogonal components of the external field in the base $\{\mathbf{i}^D, \mathbf{j}^D, \mathbf{k}^D\}$ and the outputs of the CDC-ASTRID-2 magnetometer is found by equation (12). Hence, the orthogonal base $\{\mathbf{i}^D, \mathbf{j}^D, \mathbf{k}^D\}$ established from the detector coil axes $\{\mathbf{d}_1, \mathbf{d}_2, \mathbf{d}_3\}$ define the orthogonal *magnetometer sensor axes* for the CDC, and the relation between the external magnetic field and the magnetometer offset-free components is established by a lower triangular matrix A_{CDC} . The diagonal coefficients of the matrix A_{CDC} can also be approximated to first order in the small skew terms. Thus:

$$A_{CDC} \equiv \begin{bmatrix} a_{11} & 0 & 0 \\ a_{21} & a_{22} & 0 \\ a_{31} & a_{32} & a_{33} \end{bmatrix} = \begin{bmatrix} p_1 & 0 & 0 \\ \mathbf{g}_1 p_1 & p_2 & 0 \\ \mathbf{x}_1 p_1 & \mathbf{x}_2 p_2 & p_3 \end{bmatrix} \quad (13)$$

4.2.- Cross-talk in the CDC-ASTRID-2. The previous assumption of non-mutual interaction is not, in general, valid. The proximity of the individual sensors, as depicted in figure 1a, yields to cross-talk between the individual sensors. When the sensor 1 has applied a field $-\mathbf{B}\cdot\mathbf{d}_1$ to set its own transducer to zero field, part of this field is detected by the sensor 2 because of the slight skewness and vice versa.

This effect gets enhanced if the sensors are placed close to each other and with the magnitude of the non-orthogonality. If the factor with which sensor 2 sees sensor 1 is f_{21} , the signal that sensor 2 would see (and equivalently for sensor 1, with factor f_{12} , not equal to f_{21} because of the asymmetry), is:

$$\begin{aligned}\mathbf{B}_{\text{ext}} \cdot \mathbf{d}_1 &= p_1 (\mathbf{EU}_1 - \mathbf{O}_1) - f_{12} \mathbf{B}_{\text{ext}} \cdot \mathbf{d}_2 \\ \mathbf{B}_{\text{ext}} \cdot \mathbf{d}_2 &= p_2 (\mathbf{EU}_2 - \mathbf{O}_2) - f_{21} \mathbf{B}_{\text{ext}} \cdot \mathbf{d}_1\end{aligned}\quad (14)$$

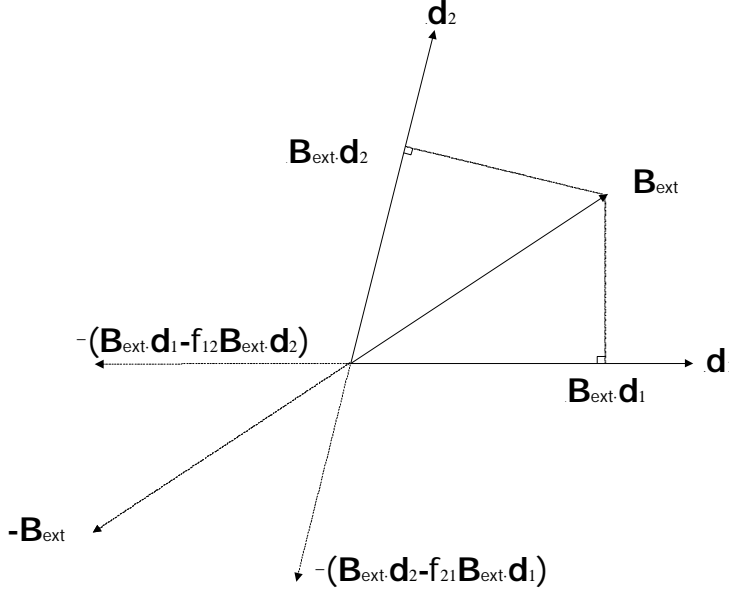


Figure 4. The *modus operandi* of the CDC (Compensation Detector Coil) sensor for the Astrid-2 satellite.

The positive factors f_{ij} are so small that 2nd order effects can be disregarded. This is a good approximation since the misalignment angles are small. A similar approach may be taken for three components, and therefore the output of each of the individual sensor axes is:

$$\begin{aligned}\mathbf{B}_{\text{ext}} \cdot \mathbf{d}_1 &\cong p_1 (\mathbf{EU}_1 - \mathbf{O}_1) - f_{12} p_2 (\mathbf{EU}_2 - \mathbf{O}_2) - f_{13} p_3 (\mathbf{EU}_3 - \mathbf{O}_3) \\ \mathbf{B}_{\text{ext}} \cdot \mathbf{d}_2 &\cong p_2 (\mathbf{EU}_2 - \mathbf{O}_2) - f_{21} p_1 (\mathbf{EU}_1 - \mathbf{O}_1) - f_{23} p_3 (\mathbf{EU}_3 - \mathbf{O}_3) \\ \mathbf{B}_{\text{ext}} \cdot \mathbf{d}_3 &\cong p_3 (\mathbf{EU}_3 - \mathbf{O}_3) - f_{31} p_1 (\mathbf{EU}_1 - \mathbf{O}_1) - f_{32} p_2 (\mathbf{EU}_2 - \mathbf{O}_2)\end{aligned}\quad (15)$$

Equation (15) is the generalization of what each individual sensor measures to first order approximation. Therefore, the relation between the magnetic field components of \mathbf{B}_{ext} and the outputs of the magnetometer is found to be expressed by the following matrix:

$$\begin{bmatrix} \mathbf{B}_1 \\ \mathbf{B}_2 \\ \mathbf{B}_3 \end{bmatrix}_{CDC} \cong \begin{bmatrix} 1 & -f_{12} & -f_{13} \\ \mathbf{g}_1 - f_{21} \mathbf{g}_2 & \mathbf{g}_2 & -f_{23} \mathbf{g}_2 \\ \mathbf{x}_1 - f_{31} \mathbf{x}_3 & \mathbf{x}_2 - f_{32} \mathbf{x}_3 & \mathbf{x}_3 \end{bmatrix} \begin{bmatrix} s_1 (\mathbf{EU}_1 - \mathbf{O}_1) \\ s_2 (\mathbf{EU}_2 - \mathbf{O}_2) \\ s_3 (\mathbf{EU}_3 - \mathbf{O}_3) \end{bmatrix} \equiv \mathbf{A}'_{CDC} \begin{bmatrix} \mathbf{EU}_1 - \mathbf{O}_1 \\ \mathbf{EU}_2 - \mathbf{O}_2 \\ \mathbf{EU}_3 - \mathbf{O}_3 \end{bmatrix}\quad (16)$$

This indicates that if the sensors are close enough a full matrix is needed to give the relationship. It is also shown that the effective detector axes will be modified. If the mutual effect between sensors is symmetric (most likely) this modification

would correspond to a rotation of the magnetic axis, otherwise a more complex system would represent the behaviour of the sensor. However, it is always possible to decompose the matrix given in equation (16) into the product of an orthogonal rotational matrix multiplied by a lower triangular matrix. This would give a system in which the *effective* magnetic axes are skew relative to the original magnetic axes existing in the case of no mutual interactions between the single transducer elements.

5.- The CSC SENSOR for the ØRSTED SATELLITE MAGNETOMETER

The Compact Spherical Coil (CSC) sensor (see figure 1b) has been implemented in the Ørsted mission and will also be used by the forthcoming CHAMP and SAC-C missions. The CSC-ØRSTED sensor consists of 3 spherical compensation coils that are perpendicular to each other, as far as the machining process can achieve. This means that the slight non-orthogonal rotational axes of symmetry will describe the 3 compensation coil axes. These axes are represented by the vectors $\{\mathbf{c}_1, \mathbf{c}_2, \mathbf{c}_3\}$ forming the skew base. The relation expressed in equation (3) indicates the deviation from orthogonality. The magnetic field \mathbf{B} inside the CSC-ØRSTED sensor will then be related to the currents in the coils by equation (8), if the offsets are neglected. Inside the spherical system there are three fluxgate transducer elements whose electronically demodulated signal is proportional to the magnetic field. Accordingly, the magnetometer feedback electronics modify the currents that are fed back to the compensation coils, so that the total magnetic field seen inside the CSC-ØRSTED is zero. This is the result of the vectorial summation between the external field \mathbf{B}_{ext} and the magnetic field applied by the compensation coils \mathbf{B} . This condition is maintained independently of possibly skew orientations of the transducer elements relative to the coil axes (Primdahl 1986).

In order to visualize the way in which the CSC-ØRSTED operates, we concentrate on the case of having only the first and second axes who define a plane. Figure 5 illustrates that the sensor compensation coils build up a field \mathbf{B} that opposes the external field \mathbf{B}_{ext} . If that were not the case, the fluxgate transducers inside the CSC would not see zero field and the zero condition provided by the feedback would break down. This also means that there is no cross-talk between the independent axes, because if the field is along a coil axis there would only be output in the corresponding channel (zero in the other two). Therefore, in the triaxial configuration the scale factors will not be changed relatively to those of each of the individual coils, as it occurs in the CDC-ASTRID-2 sensor. An approach similar to figure 5 could be taken for the full three axes system.

Consequently, the external magnetic field \mathbf{B}_{ext} is proportional to the coil currents and therefore to the outputs (in engineering units) of the magnetometer EU_i . The EU_i quantities contain an offset O_i and their conversion to nanoTesla is provided by a set of coefficients p_i . Their relation is $p_i(\text{EU}_i - O_i) = -s_i I_i$, which leads us to:

$$\mathbf{B}_{\text{ext}} = \begin{bmatrix} 1 & -\mathbf{g}_1 & \mathbf{g}_1 \mathbf{x}_2 - \mathbf{x}_1 \\ & \mathbf{g}_2 & \mathbf{g}_2 \mathbf{x}_3 - \mathbf{x}_3 \\ 0 & \frac{1}{\mathbf{g}_2} & -\frac{1}{\mathbf{g}_2} \mathbf{x}_2 \\ & \mathbf{g}_2 & \mathbf{g}_2 \mathbf{x}_3 \\ 0 & 0 & \frac{1}{\mathbf{x}_3} \end{bmatrix} \begin{bmatrix} p_1(\text{EU}_1 - \text{O}_1) \\ p_2(\text{EU}_2 - \text{O}_2) \\ p_3(\text{EU}_3 - \text{O}_3) \end{bmatrix} \equiv A_{\text{CSC}} \begin{bmatrix} \text{EU}_1 - \text{O}_1 \\ \text{EU}_2 - \text{O}_2 \\ \text{EU}_3 - \text{O}_3 \end{bmatrix} \quad (17)$$

This is similar to equation (8) and gives the relation between the orthogonal components of the external field in the base $\{\mathbf{i}^{\text{C}}, \mathbf{j}^{\text{C}}, \mathbf{k}^{\text{C}}\}$ and the outputs of the CSC-ØRSTED magnetometer are found.

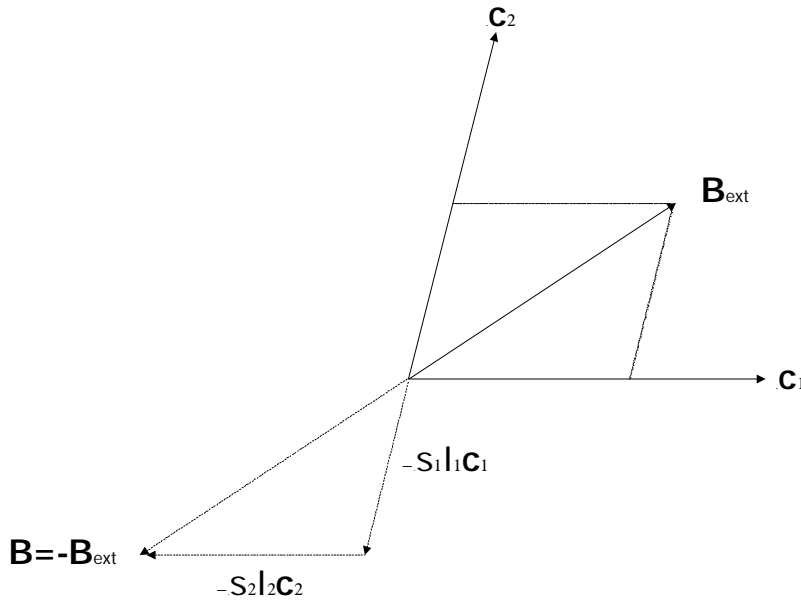


Figure 5.- The *modus operandi* of the CSC (Compensation Spherical Coil) sensor for the Ørsted satellite.

5.1.- Definition of the orthogonal magnetometer sensor axes for the CSC.

Hence, the orthogonal system in which the components of the external magnetic field \mathbf{B}_{ext} are provided for a given magnetometer are the *magnetometer sensor axes*. The orthogonal base $\{\mathbf{i}^{\text{C}}, \mathbf{j}^{\text{C}}, \mathbf{k}^{\text{C}}\}$ established from the coil axes $\{\mathbf{c}_1, \mathbf{c}_2, \mathbf{c}_3\}$ define the magnetometer axes in which the relation between the external magnetic field and the magnetometer offset-free components is an upper triangular matrix A_{CSC} . The matrix A_{CSC} can also be approximated to first order in the small skew terms by:

$$A_{\text{CSC}} \equiv \begin{bmatrix} a_{11} & a_{12} & a_{13} \\ 0 & a_{22} & a_{23} \\ 0 & 0 & a_{33} \end{bmatrix} \equiv \begin{bmatrix} p_1 & -\mathbf{g}_1 p_2 & -\mathbf{x}_1 p_3 \\ 0 & p_2 & -\mathbf{x}_2 p_3 \\ 0 & 0 & p_3 \end{bmatrix} \quad (18)$$

5.2.-The magnetic axes of the CSC sensor. The coil axes are well defined by the geometry of the CSC-ØRSTED sensor, and therefore it is possible to compute the orthogonal components of the magnetic field as function of the magnetometer outputs in the system $\{\mathbf{i}^{\text{C}}, \mathbf{j}^{\text{C}}, \mathbf{k}^{\text{C}}\}$. This is given in equation (17), in which the columns of the matrix expressing the relationship are the components of the coil axes from equation (4). Therefore, B_1 (B_2 and B_3) is formed by the contribution of all three engineering

outputs EU_i weighted by the first (second and third) component of the corresponding coil vectors $\{\mathbf{c}_1, \mathbf{c}_2, \mathbf{c}_3\}$.

The *magnetic axes* is another set of axes associated with the sensor because of their non-orthogonality character, and they represent the direction of the magnetic field \mathbf{B} for which the maximum output occurs in the sensor for a given channel. By comparison, if equation (17) is inverted, the magnetometer outputs in nanoTesla, $p_i EU_i$, can be found as functions of the orthogonal B-field components. Consequently, there exists a set of three vectors that dotted with the magnetic field \mathbf{B} , will give the coil currents, i.e. $p_i(EU_i - O_i) = \mathbf{B} \cdot \mathbf{m}_i$. These are the *magnetic axes* of the sensor and are identified as:

$$\begin{aligned} \mathbf{m}_1 &= [1, \mathbf{g}_1, \mathbf{x}_1] \\ \mathbf{m}_2 &= [0, \mathbf{g}_2, \mathbf{x}_2] \\ \mathbf{m}_3 &= [0, 0, \mathbf{x}_3] \end{aligned} \quad (19)$$

The relation between the orthogonal components of \mathbf{B} and its projections onto the coil axes can be found by dotting equation (3) with \mathbf{B} , and an equation similar to (11) is found. The magnetic axes being the columns of the transformation matrix and the projected components on the coil axes $\mathbf{B} \cdot \mathbf{c}_i$ instead of $\mathbf{B} \cdot \mathbf{d}_i$. The magnetic axes that give the maximum output in equation (17) can also be seen as the magnetic field directions relative to the coil axes in which the projection of the field onto the two other coil axes vanishes. By the use of equation (11) with $\mathbf{B} \cdot \mathbf{c}_i$ and consecutively setting two of the projected components $\mathbf{B} \cdot \mathbf{c}_i$ to zero, the magnetic axes relative to the orthogonalized system $\{\mathbf{i}^C, \mathbf{j}^C, \mathbf{k}^C\}$ are found. For completeness, the inverse of equation (11) for the coil axes ($\mathbf{B} \cdot \mathbf{c}_i$) is written here:

$$\begin{bmatrix} \mathbf{B} \cdot \mathbf{c}_1 \\ \mathbf{B} \cdot \mathbf{c}_2 \\ \mathbf{B} \cdot \mathbf{c}_3 \end{bmatrix} = \begin{bmatrix} 1 & 0 & 0 \\ -\frac{\mathbf{g}_1}{\mathbf{g}_2} & \frac{1}{\mathbf{g}_2} & 0 \\ \frac{\mathbf{g}_1 \mathbf{x}_2 - \mathbf{x}_1}{\mathbf{g}_2 \mathbf{x}_3 - \mathbf{x}_3} & -\frac{1 \mathbf{x}_2}{\mathbf{g}_2 \mathbf{x}_3} & \frac{1}{\mathbf{x}_3} \end{bmatrix} \begin{bmatrix} B_1 \\ B_2 \\ B_3 \end{bmatrix} \equiv L^{-1} \begin{bmatrix} B_1 \\ B_2 \\ B_3 \end{bmatrix} \quad (20)$$

It is easy to demonstrate that the vectors of equation (19) are neither unit vectors nor orthogonal to each other. Equation (19) shows that \mathbf{m}_3 is aligned along \mathbf{k}^C . Furthermore, each of the magnetic axes is perpendicular to the other two coil axes of different indices. And their dot product with the coil axis of the same index is one. This is expressed by:

$$\mathbf{m}_i \cdot \mathbf{c}_j \begin{cases} = 1 & j=i \\ = 0 & j \neq i \end{cases} \quad (i, j = 1, 2, 3) \quad (21)$$

However, this does not mean that \mathbf{m}_i is aligned to \mathbf{c}_i , since \mathbf{m}_i is not a unit vector. Moreover, these vectors $\{\mathbf{m}_1, \mathbf{m}_2, \mathbf{m}_3\}$ form a new skew base in three dimensional space $\{\mathbf{m}_1, \mathbf{m}_2, \mathbf{m}_3\}$. Consequently, a new orthogonal system may be constructed following the procedures of section 2.2. This new orthogonal system is denoted by $\{\mathbf{i}^M, \mathbf{j}^M, \mathbf{k}^M\}$ as opposed to the one derived from the coil axes $\{\mathbf{i}^C, \mathbf{j}^C, \mathbf{k}^C\}$.

Nevertheless, it is observed that the triad $\{\mathbf{m}_1, \mathbf{m}_2, \mathbf{m}_3\}$ could also have been derived from the coils axes as:

$$\begin{aligned}\mathbf{m}_1 &= \frac{\mathbf{c}_2 \times \mathbf{c}_3}{V_C} \\ \mathbf{m}_2 &= \frac{\mathbf{c}_3 \times \mathbf{c}_1}{V_C} \\ \mathbf{m}_3 &= \frac{\mathbf{c}_1 \times \mathbf{c}_2}{V_C}\end{aligned}\quad (22)$$

noting that the factor V_C is the volume of the parallelepiped defined by the coil axes, and it happens to be the determinant of the matrix that is formed by the triad $\{\mathbf{c}_1, \mathbf{c}_2, \mathbf{c}_3\}$. In analogy, V_M for the magnetic axes is the determinant of the matrix formed by $\{\mathbf{m}_1, \mathbf{m}_2, \mathbf{m}_3\}$. Thus:

$$\begin{aligned}V_C &= \mathbf{c}_1 \cdot (\mathbf{c}_2 \times \mathbf{c}_3) = \frac{1}{\mathbf{g}_2 \mathbf{x}_3} \\ V_M &= \mathbf{m}_1 \cdot (\mathbf{m}_2 \times \mathbf{m}_3) = \mathbf{g}_2 \mathbf{x}_3\end{aligned}\quad (23)$$

This implies that there are at least two possible sets of orthogonal reference systems that can be derived from a set of non-orthogonal coil axes. The two skew sets $\{\mathbf{c}_1, \mathbf{c}_2, \mathbf{c}_3\}$ and $\{\mathbf{m}_1, \mathbf{m}_2, \mathbf{m}_3\}$ are reciprocal or dual with respect to each other.

5.3.- Associating a reference system to the magnetic axes. As discussed, an orthogonal reference coordinate system may be constructed based on the magnetic axes. Accordingly, to first order in the small skew terms:

$$\begin{aligned}\mathbf{i}^M &\equiv \frac{\mathbf{m}_1}{|\mathbf{m}_1|} && \equiv [1, \mathbf{g}_1, \mathbf{x}_1]^T \\ \mathbf{j}^M &\equiv \frac{\mathbf{k}^M \times \mathbf{m}_1}{|\mathbf{k}^M \times \mathbf{m}_1|} && \equiv [-\mathbf{g}_1, 1, \mathbf{x}_2]^T \\ \mathbf{k}^M &\equiv \frac{\mathbf{m}_1 \times \mathbf{m}_2}{|\mathbf{m}_1 \times \mathbf{m}_2|} = \mathbf{c}_3 && \equiv [-\mathbf{x}_1, -\mathbf{x}_2, 1]^T\end{aligned}\quad (24)$$

This system is rotated relative to the system $\{\mathbf{i}^C, \mathbf{j}^C, \mathbf{k}^C\}$. There will therefore be a unitary matrix R , composed of elementary rotations that will establish the relation between the orthogonal bases $\{\mathbf{i}^C, \mathbf{j}^C, \mathbf{k}^C\}$ and $\{\mathbf{i}^M, \mathbf{j}^M, \mathbf{k}^M\}$ derived from the coil axes and the magnetic axes, respectively. The three rotation angles are (to first order) approximated by the small quantities γ_1 , ξ_1 , and ξ_2 . Thus:

$$R = R_z(\mathbf{g}_1)R_y(\mathbf{x}_1)R_x(\mathbf{x}_2) \equiv \begin{bmatrix} 1 & \mathbf{g}_1 & \mathbf{x}_1 \\ -\mathbf{g}_1 & 1 & \mathbf{x}_2 \\ -\mathbf{x}_1 & -\mathbf{x}_2 & 1 \end{bmatrix}\quad (25)$$

The orthogonal reference system derived from the magnetic axes $\{\mathbf{i}^M, \mathbf{j}^M, \mathbf{k}^M\}$ can then be found from the one derived from the coil axes $\{\mathbf{i}^C, \mathbf{j}^C, \mathbf{k}^C\}$ by applying this

rotation matrix, i.e. $\mathbf{i}^M = \mathbf{R}^T \mathbf{i}^C$, $\mathbf{j}^M = \mathbf{R}^T \mathbf{j}^C$ and $\mathbf{k}^M = \mathbf{R}^T \mathbf{k}^C$. Any magnetic field vector \mathbf{B} in the $\{\mathbf{i}^C, \mathbf{j}^C, \mathbf{k}^C\}$ system can then be transformed to the $\{\mathbf{i}^M, \mathbf{j}^M, \mathbf{k}^M\}$ system with the inverse (or transposed) of the R matrix, i.e. $\mathbf{B}_{\text{ext}}^M = \mathbf{R} \mathbf{B}_{\text{ext}}^C$.

	1	2	3
p_i	0.99865057	1.00278896	1.00441988
γ_i	-0.00145114	1.00000105	
ξ_i	0.00047535	0.00041433	1.00000019
O_i (nT)	-14.858	1.287	-31.138

Table 1. Parameter values for the Ørsted satellite magnetometer with a residual misfit of less than $0.050 \text{ nT}_{\text{RMS}}$. The magnitude of the residual offset field \mathbf{O} is 34.526 nT .

	γ_1	γ_2	ξ_1	ξ_2	ξ_3
γ_1	$2.1 \cdot 10^{-6} \cong 0$	$\gamma_1 \gamma_2 \cong \gamma_1$	$-0.7 \cdot 10^{-6} \cong 0$	$-0.6 \cdot 10^{-6} \cong 0$	$\gamma_1 \xi_3 \cong \gamma_1$
γ_2		$1 + 2.1 \cdot 10^{-6} \cong 1$	ξ_1	ξ_2	$1 + 1.2 \cdot 10^{-6} \cong 1$
ξ_1			$0.2 \cdot 10^{-6} \cong 0$	$0.2 \cdot 10^{-6} \cong 0$	ξ_1
ξ_2				$0.2 \cdot 10^{-6} \cong 0$	ξ_2
ξ_3					$1 + 0.4 \cdot 10^{-6} \cong 1$
$\sin()$	$\sin(\gamma_1) \cong \gamma_1$		$\sin(\xi_1) \cong \xi_1$	$\sin(\xi_2) \cong \xi_2$	
$\cos()$	$\cos(\gamma_1) \cong 1$		$\cos(\xi_1) \cong 1$	$\cos(\xi_2) \cong 1$	

Table 2. Cross products and trigonometrical approximations between skew and diagonal terms for the Ørsted satellite magnetometer parameters of table 1.

In order to demonstrate the validity of these approximations, a numerical example will be presented. The final calibration of the Ørsted satellite magnetometer in the coil facility of Magnetsrode at the Technical University of Braunschweig has been analyzed by the scalar calibration in Merayo *et al.* (2000), whose results adapted for the present paper are repeated in table 1. The angular values for which the axes are deviating from orthogonality (in absolute value) are 299, 98 and 86 arc sec., respectively for the inter-axes angles 12, 13 and 23.

The approximations have been made by disregarding the 2nd order in the skew terms (γ_1 , ξ_1 , and ξ_2), and setting the diagonal terms (γ_2 , and ξ_3) to one. The products between skew and diagonal terms neglect the diagonal term. Table 2 shows any possible combination and, as shown, contributions of less than 2ppm are neglected. In this table, the trigonometrical relations to the skew terms as also shown.

6.- ANGULAR REPRESENTATION of the SKEW AXES

Different approaches have been used to parametrise the skew axes as a function of the angles between the coil or magnetic axes and the orthogonal reference system axes. Merayo *et al.* (2000) use the angles between the coil axes directly since they come out automatically from computing scalar products followed by

normalization. A similar approach is used in Sabaka *et al.* (1997) denoted as type I model (Langel *et al.* 1996 and Langel 1994). It has been demonstrated above in table 1 that the diagonal coefficients are very close to one, and therefore the matrix can be approximated for either the upper or lower case by:

$$N_U \equiv \begin{bmatrix} 1 & -\mathbf{g}_1 & -\mathbf{x}_1 \\ 0 & 1 & -\mathbf{x}_2 \\ 0 & 0 & 1 \end{bmatrix}, N_L \equiv \begin{bmatrix} 1 & 0 & 0 \\ -\mathbf{g}_1 & 1 & 0 \\ -\mathbf{x}_1 & -\mathbf{x}_2 & 1 \end{bmatrix} \quad (26)$$

It is possible to compare the different parametrizations by identifying the diagonal terms n_{11} , n_{22} , n_{33} and the skewness terms n_{12} , n_{13} , n_{23} in each of the representations. In the case of an upper triangular matrix N (for the case of a lower triangular we can use N^T), the elements of N can be identified by:

$$N \equiv \begin{bmatrix} n_{11} & n_{12} & n_{13} \\ 0 & n_{22} & n_{23} \\ 0 & 0 & n_{33} \end{bmatrix} \quad (27)$$

	n_{11} =	n_{22} =	n_{33} =	n_{12} =	n_{13} =	n_{23} =	$n_{11/22/33}$ ≡	n_{12} ≡	n_{13} ≡	n_{23} ≡
Merayo <i>et al.</i> (2000)	1	$1/\gamma_2$	$1/\xi_3$	$-\gamma_1/\gamma_2$	$(\gamma_1\xi_2 - \gamma_2\xi_1)/(\gamma_2\xi_3)$	$-\xi_2/(\gamma_2\xi_3)$	1	$-\gamma_1$	$-\xi_1$	$-\xi_2$
Gödderz <i>et al.</i> (1999)	1	1	1	$-\sin\gamma_{12}$	$-\sin\gamma_{13}$	$-\sin\gamma_{23}$	1	$-\gamma_{12}$	$-\gamma_{13}$	$-\gamma_{23}$
Lühr (1999A)	1	$\cos\upsilon_{12}$	$\cos\upsilon_{13}$ $\cos\upsilon_{23}$	$\sin\upsilon_{12}$	$\sin\upsilon_{13}$ $\cos\upsilon_{23}$	$\sin\upsilon_{23}$	1	υ_{12}	υ_{13}	υ_{23}
Lühr (1999B), Sabaka <i>et al.</i> (1997) type II	1	$\cos\alpha$	$\cos\delta$	$\sin\alpha$	$\sin\delta$ $\cos\gamma$	$\sin\delta$ $\sin\gamma$	1	α	δ $\cos\gamma$	δ $\sin\gamma$
Olsen <i>et al.</i> (1999), Risbo & Olsen (1997)	1	$\cos\upsilon_1$	$\sqrt{1 - \sin^2\upsilon_2 - \sin^2\upsilon_3}$	$-\sin\upsilon_1$	$\sin\upsilon_2$	$\sin\upsilon_3$	1	$-\upsilon_1$	υ_2	υ_3
Sabaka <i>et al.</i> (1997) type I, Langel (1994)	1	$1-\gamma_1^2/2$	$\sqrt{(1-\gamma_3^2 - (\gamma_2+\gamma_1\gamma_3)^2)/(1-\gamma_1^2)}$	$-\gamma_1$	$-\gamma_3$	$-(\gamma_2+\gamma_1\gamma_3)/(1-\gamma_1^2/2)$	1	$-\gamma_1$	$-\gamma_3$	$-\gamma_2$

Table 3. Different parametrizations of the non-orthogonal angles that are found in the literature. The symbols = represent the exact expression whereas the ≡ symbol give the small-angle approximation for the given quantity.

Table 3 shows the different interpretations of the diagonal terms and skew terms independently of the orthogonal reference axes that have been used in recent publications. This table is independent of the reference system used by the given author, and it is only focusing on the definitions of the terms. It is also shown in the last four columns that in the small angle approximation valid for most cases, the terms have the same functional dependence as in Merayo *et al.* (2000). In addition, when

solving for the calibration parameters of a magnetometer, the iteration procedure tends to optimize the matrix in equation (27) until the relation for the calibrated measurements between two consecutive iterations yields an identity matrix.

7.- DISCUSSION

The relation between the physical magnetic field and the output of a space magnetometer has been presented for two different representation sensor geometries, the CSC sensor for ØRSTED satellite and the CDC sensor for the ASTRID-2 satellite. It has been demonstrated that if an orthogonal reference system is constructed based on the coil axes of the triaxial CSC sensor, then the CSC-ØRSTED features an upper triangular matrix, as opposed the system of the CDC-ASTRID-2 based on the individual detector coil axes which features a lower triangular matrix. Based on the magnetic axes the CSC-ØRSTED will also feature a lower triangular matrix, and in general an infinity of orthogonal triaxial reference systems may be chosen.

7.1.- The field applied to the magnetic sensor. In the case that the field is aligned to the coil axis \mathbf{c}_1 , the CSC-ØRSTED sensor would only produce output in the first component and also, the magnetic field for which a maximum output occurs is not aligned with \mathbf{c}_1 . In contrast, the CDC-ASTRID-2 sensor would produce outputs in all three components, and the maximum output occurs with a field aligned with the detector coil \mathbf{d}_1 . This is due to their *modus operandi*. Furthermore, if the field is aligned to the third orthogonal axis \mathbf{k}^C , the CSC-ØRSTED will give output in all three components (with almost all the field in the third axis), whereas the CDC-ASTRID-2 would give only field in the third component. This can be easily seen when using the relationships given in equations (17) and (20).

7.2.- Connection with the spherical harmonic thin shell method. The spherical harmonic method was developed to study the sensor response when a magnetic field is applied in different directions at constant magnitude, called the thin shell method (Merayo *et al.* 1995, Risbo and Olsen 1996 and Risbo 1999). Not only the linear response is determined but also the transverse and axial non-linearities of the sensor. It is based on the expansion in spherical harmonic functions of any of the magnetometer outputs. The terms of degree $n=1$ represent the linear response whereas the non-linear responses are described by terms of higher degree. If we only concentrate on the linear terms, i.e. $n=1$, the output of any of the magnetometer channels EU_i , disregarding the offset O_i , can be written as the dot product of a directional vector \mathbf{q}_i and the external magnetic field \mathbf{B}_{ext} , i.e. $EU_i = \mathbf{B}_{\text{ext}} \cdot \mathbf{q}_i$. Consequently, there will be a set of three coefficients (the three components of \mathbf{q}_i) for each channel. These vectors \mathbf{q}_i represent the directions of the magnetic axes \mathbf{m}_i of the magnetometer in the reference system in which \mathbf{B}_{ext} is expressed. Hence, a rotational matrix Q exists that transforms the system into the triad $\{\mathbf{i}^M, \mathbf{j}^M, \mathbf{k}^M\}$, and so the relation between the magnetometer outputs and the external magnetic field for the CSC-ØRSTED in this case is given by:

$$\mathbf{B}_{\text{ext}}^M = \begin{bmatrix} 1 & 0 & 0 \\ \mathbf{g}_1 & \mathbf{g}_2 & 0 \\ \mathbf{x}_1 & \mathbf{x}_2 & \mathbf{x}_3 \end{bmatrix} \begin{bmatrix} p_1(\text{EU}_1 - \text{O}_1) \\ p_2(\text{EU}_2 - \text{O}_2) \\ p_3(\text{EU}_3 - \text{O}_3) \end{bmatrix} \equiv A_{\text{CSC}}^M \begin{bmatrix} \text{EU}_1 - \text{O}_1 \\ \text{EU}_2 - \text{O}_2 \\ \text{EU}_3 - \text{O}_3 \end{bmatrix} \quad (28)$$

It uses the orthogonal system derived from $\{\mathbf{m}_1, \mathbf{m}_2, \mathbf{m}_3\}$, as opposed to equation (18) which uses the orthogonal system derived from the coil axes $\{\mathbf{c}_1, \mathbf{c}_2, \mathbf{c}_3\}$.

7.3.- Representation selection. Both the lower and the upper triangular matrix representations for the relation between the magnetometer outputs and the orthogonal components are equally valid. However, once the representation has been chosen it has a consequence for the interpretation of the reference system, which has to be consistent according to the application. Apart from the references already mentioned, there are other authors who use a representation for the magnetometer (Brauer *et al.* 1999, Jørgensen *et al.* 1999, Primdahl *et al.* 1999, Zheng *et al.* 1999, Merayo *et al.* 1998 and Brauer 1997). Some give a definition of which reference system is used for constructing the relationship matrix, others do not mention it because an orthogonal reference system magnetic field vector will be provided from their observations. It is in fact possible to determine an orthogonal reference system that lies between the ones derived from the coil axes and from the magnetic axes in order to obtain minimum non-orthogonality angles between the components. In principle there are an infinite number of orthogonal systems that can be used as base for our observations.

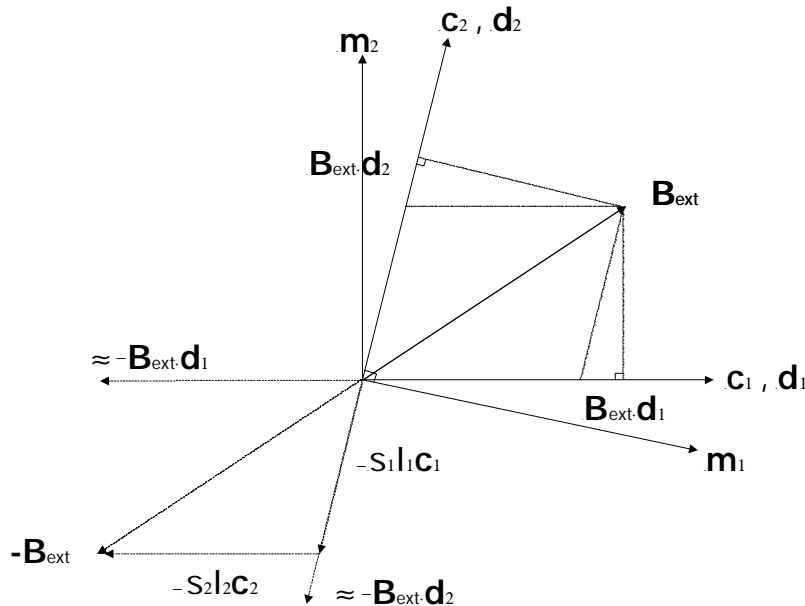


Figure 6.- The two sets of axes (in the plane) that can be employed for representing the physical magnetic field that is measured by a magnetometer: The coil axes $\{\mathbf{c}_1, \mathbf{c}_2\}$ for the ØRSTED-CSC sensor or the detector coil axes $\{\mathbf{d}_1, \mathbf{d}_2\}$ for the ASTRID-2-CDC sensor and the magnetic axes $\{\mathbf{m}_1, \mathbf{m}_2\}$ are shown.

7.4.- The reciprocal systems. The two representations that have been described so far are explained in a general sense by using Tensor Algebra. However, the tensorial terms have been omitted in order not to complicate the natural existence of two sets of coordinates and basis, dual or reciprocal from each other, when treating non-orthogonal systems. Figure 6 combines the two representations as emerged from figures 4-5. The currents in the compensation coils are the contravariant components

of the magnetic field vector in the coil axes and the covariant components in the magnetic axis.

8.- CONCLUSION

It is up to the calibration team to decide which representation suits better a given experiment. The basic topologies for magnetic systems are illustrated in table 4, although there exists an infinite number of possibilities. However, care should be taken when interchanging parameters. It is more convenient to give the transformation matrix as the information inherent to a magnetometer instead of using a basis whose physical meaning is obscure or disjointed. Since it is possible misinterpreting the calibration parameters for example using an upper matrix when the parameters have been derived with a lower matrix representation.

In this case, the error in the orientation of the magnetometer Ψ with respect to an absolute reference system (given by a star imager) is proportional to the root-square-sum of all the non-orthogonality angles and that can be derived from equation (25). This angle is:

$$\Psi = \sqrt{g_1^2 + x_1^2 + x_2^2} \quad (29)$$

	Coil axes $\{\mathbf{c}_1, \mathbf{c}_2, \mathbf{c}_3\}$	Detector Coil axes $\{\mathbf{d}_1, \mathbf{d}_2, \mathbf{d}_3\}$	Magnetic axes $\{\mathbf{m}_1, \mathbf{m}_2, \mathbf{m}_3\}$
Coil System	Upper	-	-
CSC-ØRSTED	Upper	-	Lower
CDC-ASTRID-2	-	-Lower	Lower

Table 4. Functional matrix topology for orthogonalization of a magnetometer that is determined from the orthogonal system chosen.

There are some disadvantages on using the magnetic axes, since the orthogonal system will change in the event of disconnecting any of the individual element transducers. On the contrary, this would not occur for the orthogonal reference system derived from the coil axes. However, the detector coil axes for the CDC-ASTRID-2 give some trouble since its inherent intercoupling between axes produce a full matrix.

The Ørsted satellite calibration programme is based on the magnetic axes of the sensor even though there exists the opportunity of establishing the magnetic observations on the coil axes. Regardless of the advantages of the upper matrix representation, the lower matrix is used instead because it is as valid as its upper counterpart. Also, the science group has used the lower representation since the beginning of the project and it would not have made sense at this late stage to change

any working calibration programs, or well-tested and reliable subroutines. Because it will not have impact in the instrumental performance and/or science results.

9.- ACKNOWLEDGEMENTS

The authors thanked the Ørsted satellite project team and the Danish sponsoring agencies. Professor Hermann Lühr from Potsdam-GFZ is also thanked for being involved in many discussions about this paper.

10.- REFERENCES

Acuña, M.H., C.S. Scarce, J.B. Seeck and J. Scheifele; *The MAGSAT Vector Magnetometer – A Precision Fluxgate Magnetometer for the Measurement of the Geomagnetic Field*, NASA Technical Memorandum 79656, October 1978

Acuña, M.H.; *MAGSAT – Vector Magnetometer Absolute Sensor Alignment Determination*, NASA Technical Memorandum 79648, September 1981

Brauer, P., J.M.G. Merayo, T. Risbo and F. Primdahl, *Magnetic calibration of vector magnetometers: linearity, thermal effects and stability*, Workshop on Calibration of Space-Borne Magnetometers, Institute of Geophysics and Meteorology, Technical University of Braunschweig, March 9, 1999, submitted to ESA-SP, 2000

Brauer, P., T. Risbo, J.M.G. Merayo and O.V. Nielsen, *Fluxgate sensor for the vector magnetometer onboard the "Astrid-2" satellite*, Sensors and Actuators, A Physical, A 60, (accepted), 1998

Brauer, P., *The Ringcore fluxgate sensor*, Ph.-D. thesis DTU, 135pp. 1997

Brauer, P., J.M.G. Merayo, O.V. Nielsen, F. Primdahl and J.R. Petersen, *Transverse field effect in fluxgate sensors*, Sensors and Actuators, A Physical, A 59, 70-74, 1997

Gödderz, K., H. Lühr, M. Rother and R. Bock, *CHAMP Optical Bench Star Camera/Vector Magnetometer Inter-Calibration*, Workshop on Calibration of Space-Borne Magnetometers, Institute of Geophysics and Meteorology, Technical University of Braunschweig, March 9, 1999, submitted to ESA-SP, 2000

Jørgensen, P.S., P. Brauer, J.M.G. Merayo, N. Olsen and F. Primdahl, *In-Flight Calibration of Rocket Borne Vector Magnetometer Data*, Workshop on Calibration of Space-Borne Magnetometers, Institute of Geophysics and Meteorology, Technical University of Braunschweig, March 9, 1999, submitted to ESA-SP, 2000

Langel, R.A., J.A. Conrad, T.J. Sabaka and R.T. Baldwin, *Adjustment of UARS, POGS, and DE-1 Satellite Magnetic Field Data for Modelling the Earth's Main Field*, J. Geomag. Geoelectr., 48, 1996

Langel, R.A., *Suggested procedures for in-flight calibration of the Ørsted vector magnetometer*, private communication, 7/11-1994

Lühr, H., private communication in fax, 26/10-99A

Lühr, H., private communication in fax, 12/10-99B

Merayo, J.M.G., P. Brauer, F. Primdahl, J.R. Petersen and O.V. Nielsen, *Scalar calibration of vector magnetometers*, Meas. Sci. Technol., 11, 120-132, 2000

- Merayo, J.M.G., P. Brauer, F. Primdahl and J.R. Petersen, *Absolute magnetic calibration and alignment of vector magnetometers in the Earth's magnetic field*, Workshop on Calibration of Space-Borne Magnetometers, Institute of Geophysics and Meteorology, Technical University of Braunschweig, March 9, 1999, submitted to ESA-SP 1999A
- Merayo, J.M.G., *Magnetic Gradiometry*, Ph.D. thesis, Technical University of Denmark, 1999B
- Merayo, J.M.G., P. Brauer, T. Risbo, E.B. Pedersen, J.R. Petersen and F. Primdahl, *Astrid-2 EMMA magnetic calibration*, Astrid-2 satellite technical note, Department of Automation, Technical University of Denmark, 1998
- Merayo, J.M.G., T. Risbo, F. Primdahl, O.V. Nielsen, and J.R. Petersen, *Calibration of the fluxgate CSC vector magnetometers "Flight" model and "Flight Spare" model for the Ørsted satellite*, Ørsted Satellite Project, Technical Note #278, 1995
- Nielsen, O.V., P. Brauer, F. Primdahl, T. Risbo, J.L. Jørgensen, C. Boe, M. Deyerler and S. Bauereisen, *A high-precision triaxial fluxgate sensor for space applications: layout and choice of materials*, Sensors and Actuators, A Physical, A 59, 168-176, 1997
- Nielsen, O.V., J.R. Petersen, F. Primdahl, P. Brauer, B. Hernando, A. Fernández, J.M.G. Merayo and P. Ripka, *Development, construction and analysis of the "Ørsted" fluxgate magnetometer*, Meas. Sci. Technol., 6, 1099-1115, 1995
- Olsen, N., T. Risbo, P. Brauer, J.M.G. Merayo, F. Primdahl and T. Sabaka, *Calibration of the Ørsted Vector Magnetometer*, Workshop on Calibration of Space-Borne Magnetometers, Institute of Geophysics and Meteorology, Technical University of Braunschweig, March 9, 1999, submitted to ESA-SP, 2000
- Pedersen, E.B., F. Primdahl, J.R. Petersen, J.M.G. Merayo, P. Brauer and O.V. Nielsen, *Digital fluxgate magnetometer for the Astrid-2 satellite*, Meas. Sci. Technol., 10, 124-9, 1999
- Primdahl, F., P. Brauer, J.M.G. Merayo, J.R. Petersen and T. Risbo, *Determining the direction of a geometrical/optical reference axis in the coordinate system of a tri-axial magnetic sensor*, Workshop on Calibration of Space-Borne Magnetometers, Institute of Geophysics and Meteorology, Technical University of Braunschweig, March 9, 1999, submitted to ESA-SP, 2000
- Primdahl, F., H. Lühr and E.K. Lauridsen, *The effect of large uncompensated transverse fields on the fluxgate magnetic sensor output*, DRI 1-92, Danish Space Research Institute, 1992
- Primdahl, F., *Instrumentos Geomagnéticos*, Publicações do Observatório Nacional do Brasil n°09, 76pp., 1986
- Primdahl, F. and P. Anker Jensen, *Compact spherical coil for fluxgate magnetometer vector feedback*, J. Phys. E: Sci. Instrum. 15, 221-226, 1982
- Risbo, T., P. Brauer, J.M.G. Merayo, O.V. Nielsen, J.R. Petersen, F. Primdahl and N. Olsen, *Calibration of the Ørsted Space Vector Magnetometer with Coil Test Systems*, Workshop on Calibration of Space-Borne Magnetometers, Institute of Geophysics and Meteorology, Technical University of Braunschweig, March 9, 1999, submitted to ESA-SP, 2000
- Risbo, T. and N. Olsen, *Attitude Intercalibration of the Star Imager and the Spherical Compact Sensor Magnetometer for the Ørsted Geomagnetic Satellite Mission*, SPIE Proceedings v. 2810, 230-238, 1996
- Sabaka, T., J.A. Conrad, J.M.G. Merayo and R.A. Langel, *Analysis of Defense Meteorological Satellite Program 12 and 13 Satellite Magnetometer Measurements*, GSFC-NASA contract NAS5-31760, 1997
- Zheng, Y., K.A. Lynch and M. Boehm, *Magnetic Field Data Analysis of 4 Free-Flyer Magnetometers*, submitted to ESA-SP, 2000